Received: 21 November 2023 | Revised: 6 February 2024 | Accepted: 4 March 2024

DOI: 10.1002/mrc.5444

RESEARCH ARTICLE

WILEY

DFT investigation of coupling constant anomalies in substituted β-lactams

Emily B. Crull[1] | **Alexei V. Buevich**[2] | **Gary E. Martin**[3] | **Rohit Mahar**[4,5] | **Bo Qu**[4] | **Chris H. Senanayake**[4] | **Tadeusz F. Molinski**[6,7] | **R. Thomas Williamson**[1]

[1]Department of Chemistry and Biochemistry, University of North Carolina Wilmington, Wilmington, North Carolina, USA

[2]Analytical Research and Development, Merck & Co, Inc, Rahway, New Jersey, USA

[3]Department of Chemistry and Biochemistry, Seton Hall University, West Orange, New Jersey, USA

[4]TCG GreenChem, Inc, Ewing, New Jersey, USA

[5]Current address: Department of Chemistry, Hemvati Nandan Garhwal University, (A Central University), Srinagar, Uttarakhand, India

[6]Department of Chemistry and Biochemistry, University of California San Diego, La Jolla, California, USA

[7]Skaggs School of Pharmacy and Pharmaceutical Sciences, University of California San Diego, La Jolla, California, USA

Correspondence
R. Thomas Williamson, Department of Chemistry and Biochemistry, University of North Carolina Wilmington, Wilmington, NC 28409, USA.
Email: williamsonr@uncw.edu

Funding information
National Science Foundation, Grant/Award Numbers: CHE0821552, CHE2116395

Abstract

β-lactams are a chemically diverse group of molecules with a wide range of biological activities. Having recently observed curious trends in $^{2}J_{HH}$ coupling values in studies on this structural class, we sought to obtain a more comprehensive understanding of these diagnostic NMR parameters, specifically interrogating $^{1}J_{CH}$, $^{2}J_{CH}$, and $^{2}J_{HH}$, to differentiate 3- and 4-monosubstituted β-lactams. Further investigation using computational chemistry methods was employed to explore the geometric and electronic origins for the observed and calculated differences between the two substitution patterns.

KEYWORDS

electrostatic potential, Fermi contact, PIP-HSQC, PIP-HSQMBC, scalar couplings, β-lactams

1 | INTRODUCTION

β-lactams, chemically known as azetidin-2-ones, are four-membered cyclic lactams.[1] β-lactams exhibit a host of biological activities, most notably potent antibacterial activity, though the list also includes anticonvulsant, anticancer, antidiabetic, and anti-inflammatory properties.[1,2] Members of his class of compound are also indicated for the treatment of Parkinson's disease.[1,2] Because of increasing prevalence of antibiotic resistance, there is persistent interest in the evaluation of novel derivatives of this structural class and others to supplement the available penicillin, cephalosporin, and monobactam analogs now widely used to treat infections.[3,4] This continuing interest mandates a deeper understanding of the structural characteristics of the precursors to more complex variants.

NMR is a cornerstone in the structural analysis of organic compounds. While a host of NMR data exists pertaining to the chemical shifts of natural and synthetic β-lactams, far less is known about the scalar coupling constants of this structural class. What information does exist generally emphasizes the ^{1}H-^{1}H couplings without any mention of the $^{n}J_{CH}$ couplings. In the mid-1960s, an unusual and diagnostic geminal coupling constant was observed that can distinguish between the substituted Types A and type B β-lactams shown in Figure 1.[5] Geminal ^{1}H-^{1}H couplings observed for type A compounds were reported to be approximately 14 Hz, while those of type B analogs exhibited geminal couplings of less than 6 Hz.[5–7] To our knowledge, no further examination of the generality of these scalar couplings or other possible anomalies in the scalar couplings of β-lactams has been reported.

Since that early study, this often overlooked NMR parameter has been used to elucidate some challenging marine natural product structures.[8–10] In the early 1990s, a novel macrolactam, discodermide, was isolated from *Discodermia dissoluta*, and the structure was observed to have the aforementioned large geminal ^{1}H-^{1}H couplings for the amide adjacent CH_2.[8] These couplings were also used to identify the AB quartet of the diastereotopic *O*-benzyloxy protons of a synthetic chiral analog of bastadin 5, a macrolactam natural product from the marine sponge *Ianthella basta*.[9] The hexahydro-1*H*-isoindolone ring of muironolide A, a natural product from a new *Phorbas* species, was assigned from the magnitude of the geminal ^{1}H-^{1}H coupling within the g-lactam ring.[10] The variety of these examples underscores the need for better understanding of these scalar coupling trends.

To probe these diagnostic NMR parameters, a set of mono-substituted β-lactams was assembled, featuring small achiral R-groups with limited flexibility (Figure 1). Two of these compounds were analyzed spectroscopically (Figure 2), and all compounds were concurrently evaluated with modern computational chemistry techniques. The analysis has revealed several interesting trends that can be divided into two categories: those that can be used to differentiate signals within one type of β-lactam and those that can be used to differentiate between the two types of β-lactams.

2 | COMPUTATIONAL METHODOLOGY

Conformers were generated using the MacroModel conformational search.[11] Those molecules with multiple conformers were averaged using Boltzmann weighting derived from the calculated energies. The geometry optimizations, energy calculations, and NMR calculations were then conducted using Gaussian 16 (output files as part of the supporting information).[12] Geometry optimizations, energy calculations, and NMR calculations were all performed at the B3LYP/6–311 + G(2d,p) level.[12] The hybrid B3LYP functional was chosen due to its prolific use and the high accuracy to predict geometries, energies, and NMR chemical shift and *J*-coupling parameters.[13–15] The calculations were done in gas phase, as the two sets of experimental data presented in this work were acquired in chloroform, which has limited solvent effects.[13] The scalar coupling constants were calculated with the Gaussian keyword "NMR = mixed." The NMR mixed keyword implements the use of two different bases sets to improve the accuracy of spin–spin coupling constants by using uncontracted basis functions for the Fermi contact, most dominant component of the scalar coupling, and a contracted basis set, which is faster but less accurate, for the remaining three components, the spin-dipolar, paramagnetic spin-orbital, and diamagnetic spin-orbital contributions. However, as these are minor components, the loss in accuracy in exchange for

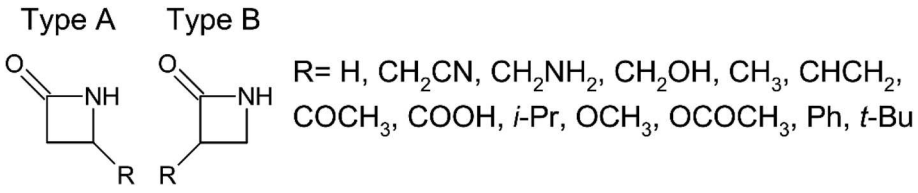

FIGURE 1 The two types of mono-substituted β-lactams and the R groups that composed the set of molecules analyzed in this study.

decreased computation time is acceptable.[15,16] The mixed method uses the default setting, Grid = UltraFine, which includes 95 radial shells and 590 angular points per shell.[15,16] Overall, the "mixed" approach requires more computation time, but it is more accurate than the direct "spinspin" calculations.

3 | EXPERIMENTAL OBSERVATIONS

The $^{n}J_{HH}$ couplings were extracted from the ^{1}H NMR spectra (Figure 2) of exemplars from each type of lactam; the scalar couplings of the CH and CH_2 resonances are collected in Table 1. These values generally agreed well with the computed values, with an MAE of 0.6 Hz. The $^{n}J_{CH}$ couplings were determined experimentally using the PIP-HSQC[16] and/or PIP-HSQMBC[16] experiments and are reported in Table 2. The $^{1}J_{CH}$ coupling constants exhibited an MAE of 3.0 Hz, while the longer range $^{n}J_{CH}$ couplings had an MAE of 0.6 Hz. Given the larger overall values of $^{1}J_{CH}$ couplings, this is a proportionally smaller deviation than was observed for $^{n}J_{CH}$ couplings.

There are two trends observed on a structure-by-structure basis. First, the $^{1}J_{CH}$ for C4 is larger than the $^{1}J_{CH}$ for C3 (~151 vs. ~144 Hz), regardless of which is

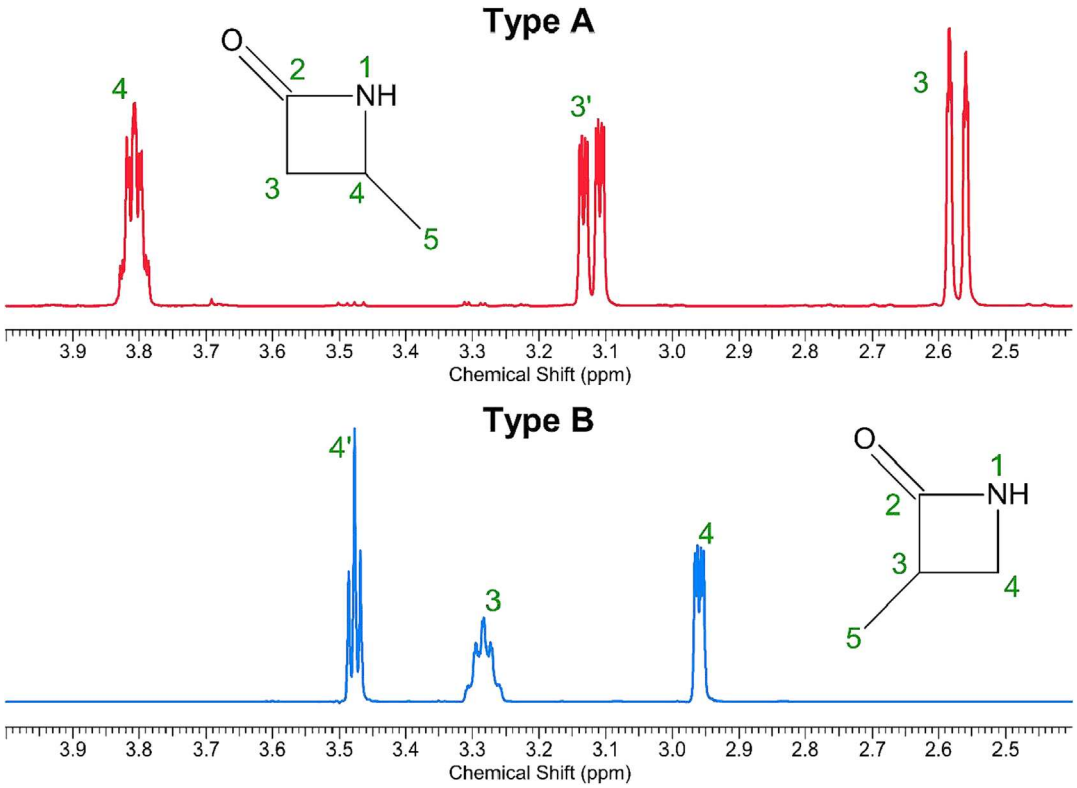

FIGURE 2 Expansions of the experimental ^{1}H NMR spectra ($CDCl_3$) of the two types of methyl substituted β-lactams (full spectra available in the supporting information).

TABLE 1 Summary of the experimental (signs not determined) and computed $^{n}J_{HH}$ coupling constants with the absolute difference (Abs. Δ) for Types A and B molecules with R = Me (refer to Figure 2).

Type A				Type B			
J_{HH}	Experimental (Hz)	Computed (Hz)	Abs. Δ (Hz)	J_{HH}	Experimental (Hz)	Computed (Hz)	Abs. Δ (Hz)
3–3′	−14.8	−15.4	0.6	4–4′	−5.3	−5.3	0.1
1–3	−1.4	−0.3	1.1	1–3	<1.5	0.6	NC
1–3′	2.0	3.2	1.2	1–4	<1.5	−0.8	NC
1–4	<1.5	−0.1	NC	1–4′	<1.5	−1.2	NC
3–4	2.2	2.3	0.0	3–4	2.4	2.3	0.2
3′-4	5.0	5.8	0.9	3–4′	5.3	5.9	0.6

Abbreviation: NC, not calculated.

TABLE 2 Summary of $^{n}J_{CH}$ and $^{1}J_{CH}$ coupling constants for Types A and B molecules with R = Me (refer to Figure 2), with the computed values listed first, followed by the experimental (signs not determined) and then the absolute difference between the two.

Type A heteronuclear couplings (Hz)						Type B heteronuclear couplings (Hz)					
		Carbon						Carbon			
		2	3	4	5			2	3	4	5
Proton	3	−5.8	144.2	−2.6	3.8	Proton	3	−5.7	142.0	−1.7	2.5
		−6.3	139.4	−3.8	4.0			−6.0	138.6	−1.1	2.0
		0.5	4.8	1.2	0.2			0.3	3.5	0.6	0.5
	3′	−5.5	144.4	−1.1	1.6		4	2.8	−2.3	151.3	−4.0
		−5.3	139.3	−2.2	1.6			2.8	−2.3	153.0	−3.7
		0.2	5.1	1.1	0.0			0.0	0.0	1.6	0.3
	4	2.6	−1.1	150.1	−3.5		4′	4.9	−1.5	151.6	−1.7
		3.2	−1.6	150.0	−2.5			5.1	−2.6	150.0	−1.6
		0.6	0.5	0.1	1.0			0.2	1.1	1.6	0.1
	5	0.6	5.0	−6.6	130.0		5	6.7	3.8	−6.6	131.4
		1.5	4.8	−5.0	126.0			6.8	2.7	−6.9	128.0
		0.9	0.2	1.6	4.0			0.1	1.1	0.3	3.4

the methylene and which is the methine. Exceptions to this rule for Type B compounds will be discussed later in the text. Second, the magnitude of $^{2}J_{CH}$ between C2 and H3/H3′ is always greater than $^{2}J_{CH}$ between C4 and H3/H3′ (∼ −5.6 vs. −[2.3–1.1] Hz). It is important to note that both trends are also observed in the unsubstituted β-lactam, implying that these trends are intrinsic to the structure itself, rather than a consequence of the substitution pattern.

Comparing the computed values of both chemical shifts and scalar coupling constants, for Types A and B compounds, multiple trends emerge. Regarding the calculated ^{1}H spectra, the CH proton resonance in Type A molecules is observed further downfield than for the corresponding Type B analog. Conversely, for the ^{13}C spectra, the carbon resonance for C2 for Type A is observed further upfield than for Type B unless a carbonyl is the first structural component of the substituent attached to the ring. The most apparent trend is seen in the relative size of the geminal coupling for the CH_2 protons. The geminal coupling between the Type A protons at C3 was 8 to 11 Hz larger in magnitude than the corresponding values at the C4 position in Type B compounds. Differences between the geminal coupling at the 3- and 4-positions are also observed in the unsubstituted β-lactam, again suggesting that the difference in the magnitude of the coupling constants are intrinsic to the structure due to the local electronic environment and not a consequence of the substitution pattern.[6,7] Turning to the $^{1}J_{CH}$ couplings, the methine $^{1}J_{CH}$ coupling of a Type A molecule (C4) is larger than the corresponding methine heteronuclear coupling of type B (C3) compounds, while the reverse is true for the $^{1}J_{CH}$ couplings of the CH_2 (Type B > Type A). These two trends arise directly from the $^{1}J_{CH}$ of C4 being greater than the $^{1}J_{CH}$ of C3, though exceptions to that trend are not exceptions to the trends between types.

4 | OTHER OBSERVATIONS

A few other interesting observations were made during this study, the more significant of which is that differences in $^{1}J_{CH}$ and $^{2}J_{HH}$ couplings between the C3 and C4 sites are also present in an unsubstituted β-lactam. This observation suggests that experimental differences are primarily associated with the β-lactam moiety itself and not a function of the substituents. Also notable is the fact that the Fermi contact formula contains a term for the electron magnetic dipole moment, thereby implying that it is directly influenced by the electronegativity of the atoms in question (see Figures 3–5).[17] The Fermi contact correlates extremely well with the J values, with all examined couplings exhibiting R^2 values of >0.999. Consequently, exploring the electron density of the system and the individual atoms was a logical place to start looking for an explanation to such trends.[18,19]

5 | POSSIBLE ORIGINS FOR THE *J* DISPARITY

There is insufficient variation in the calculated bond lengths and angles to explain the differences observed in

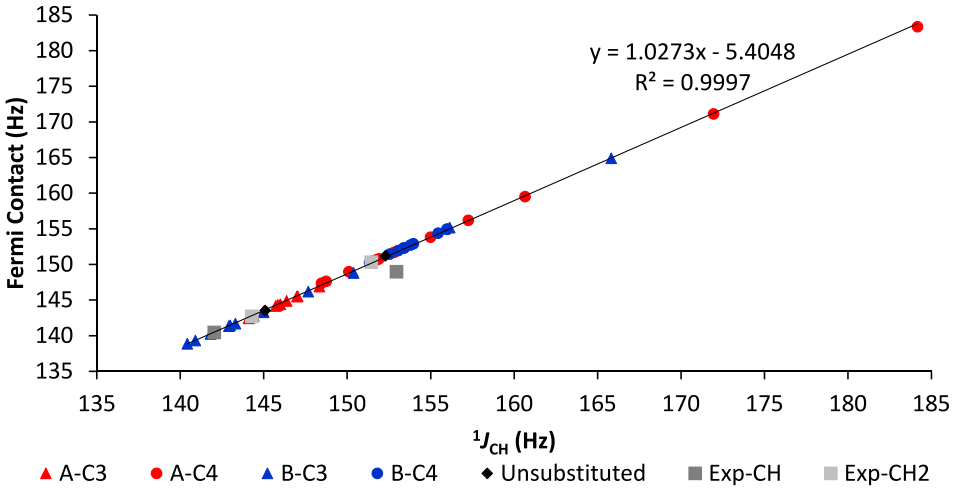

FIGURE 3 The correlation of the DFT-calculated Fermi contact versus the DFT-calculated and experimentally measured for R = Me (see Figure 2) $^{1}J_{CH}$ coupling. *J*-coupling values for methylene pairs are averaged. The equation and R^2 do not include the experimental data.

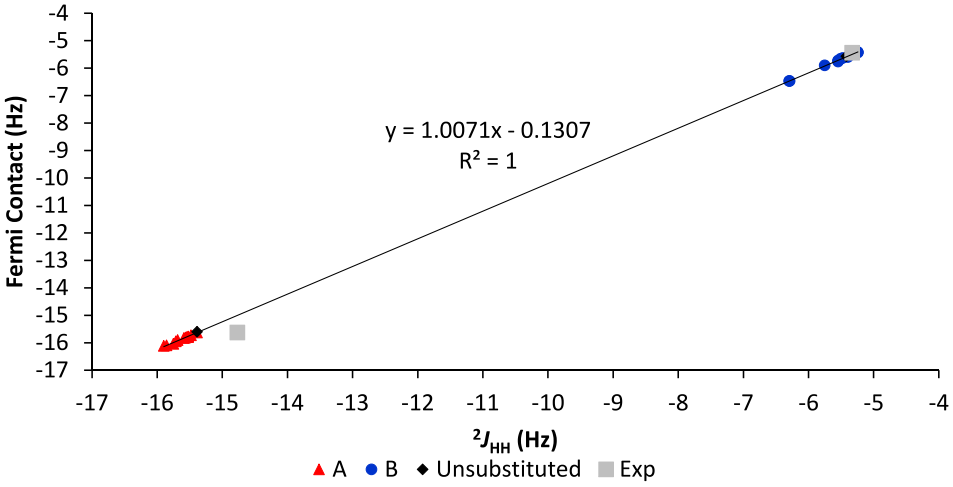

FIGURE 4 The Fermi contact contribution to the DFT-computed and experimentally measured for R = Me (see Figure 2) $^{2}J_{HH}$ coupling correlated to the $^{2}J_{HH}$ value. The equation and R^2 do not include the experimental data.

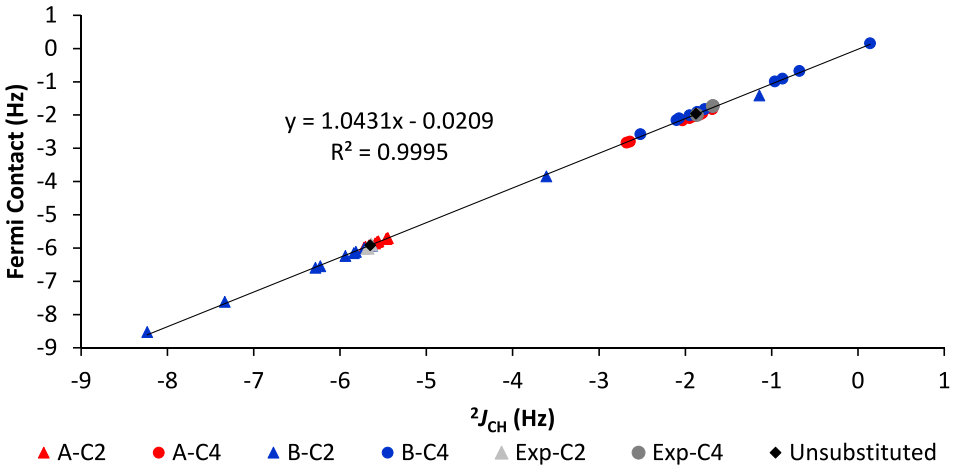

FIGURE 5 The average Fermi contact contribution correlated to the average DFT-calculated and experimentally measured for R = Me (see Figure 2) $^{2}J_{CH}$ values for carbons 2 and 4 from H3/H3′. The equation and R^2 do not include the experimental data.

the scalar couplings. Thus, the focus must shift from geometric considerations to the electronic properties of β-lactams. When exploring the structure of β-lactams, it was found that the partial double bond character of O=*C-N* decreases the electron density on nitrogen (Figure 6).[6] Analogous behavior has also been reported for lactones, albeit to a lesser extent, leading us to conclude that the vicinal nitrogen produced less of an effect than cases where there is an oxygen at this position.[6,7] Similarly, the partial double bond character (O=C-N), caused by both the delocalization of electron density towards the carbonyl bond and electron donation from the nitrogen, could also be responsible for changes in the magnitude of the $^{n}J_{CH}$ couplings. In this case, the ability of the carbonyl (C2) to extract electron density from the nitrogen (N1) amplifies the ability of the nitrogen atom to withdraw electron density from C4. The same trend would be observed with β-lactones, β-thiolactams, and other ring systems with similar geometries, albeit to varying degrees depending on the level of electronegativity and conjugation. This charge redistribution is numerically represented by the so-called electrostatic potential (ESP) of the atom.

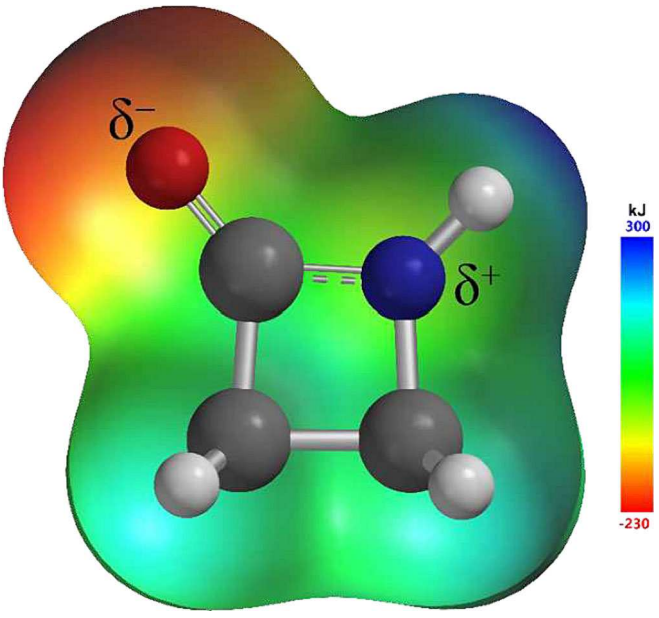

FIGURE 6 Electrostatic potential map computed at the B3LYP/6–311 + G(2d,p) level (IsoValue of 98%)[20] showing the nitrogen lone pair contribute to the C2-N1 bond causing the observed charge distribution. It should be noted that no correlation was identified between the $^{2}J_{HH}$, $^{1}J_{CH}$, or $^{2}J_{CH}$ scalar couplings and the C2-N1 bond lengths (descriptive plots available in the supporting information).

6 | DISPARITY IN $^{1}J_{CH}$ BETWEEN TYPES A AND B COMPOUNDS

One of the most convenient NMR parameters to measure, and perhaps theoretically the simplest to understand, is the $^{1}J_{CH}$ scalar coupling. That the magnitude of $^{1}J_{CH}$ is proportional to % s-character of the hybridized orbitals that comprise sigma bonds (Figure 7) is well established, but the size of the coupling constant also depends on host of other factors, such as substitution and stereoelectronic effect (ring strains).[21] Since this work is examining the same base ring structure in each case, ring strain was not addressed in this work. The %s character of the sp^3-carbon atoms, such as the ones studied here, could be dependent on the electronegativity of the substituent atoms and would thus be potentially correlated to ESP. The lower electron density at C4 compared to C3 caused by the electronegativity of nitrogen atom agrees with the trend in ESPs, wherein C4 generally has more positive ESP than C3 (Figure 8). Note how for each Types A and B molecule, the CH_2 carbon values display less distribution of ESP than the those of the CH and furthermore, how the unsubstituted analog sits in the corner of the slanted "L-shaped" distribution (Figure 8). Additionally, the two outermost points for each type are when the R-group is attached to the ring through an oxygen atom, and the methine $^{1}J_{CH}$ coupling constants are more dispersed due to the substitution effect compared with methylene $^{1}J_{CH}$ coupling constants (Figure 9).[22] The correlation between electron density and $^{1}J_{CH}$ can be expressed by comparing the ESPs of the carbons (with the hydrogens summed in) versus the $^{1}J_{CH}$ values, which show a linear correlation for each A/B and C4/C3 pair (Figure 10). These data suggest that the presence of electronegative nitrogen in β-lactams causes an increase in the magnitude of $^{1}J_{CH}$ of the adjacent C4 carbon. This change in electron density is consistent with the observation that $^{1}J_{CH}$ for the C4 is generally larger than that of C3. An exception to this rule occurs when the R-group is itself an electron withdrawing substituent on C3. In this case, when the R-group is connected to C3 via oxygen, the inductive effects of the oxygen play a major role in increasing the magnitude of the $^{1}J_{CH}$ coupling constant of C3. The correlation between electron density and coupling constants also agrees with Cookson's observation that as the ring size increases, the magnitude of the geminal coupling of the CH_2 adjacent to the heteroatom increases, closer to nominal magnitude, such as observed at α-CH_2.[6,7] The increase in ring size would provide increases in the bond path and thus insulate CH_n from inductive electron withdrawal, thereby reducing the magnitude of the $^{1}J_{CH}$ scalar coupling constant.

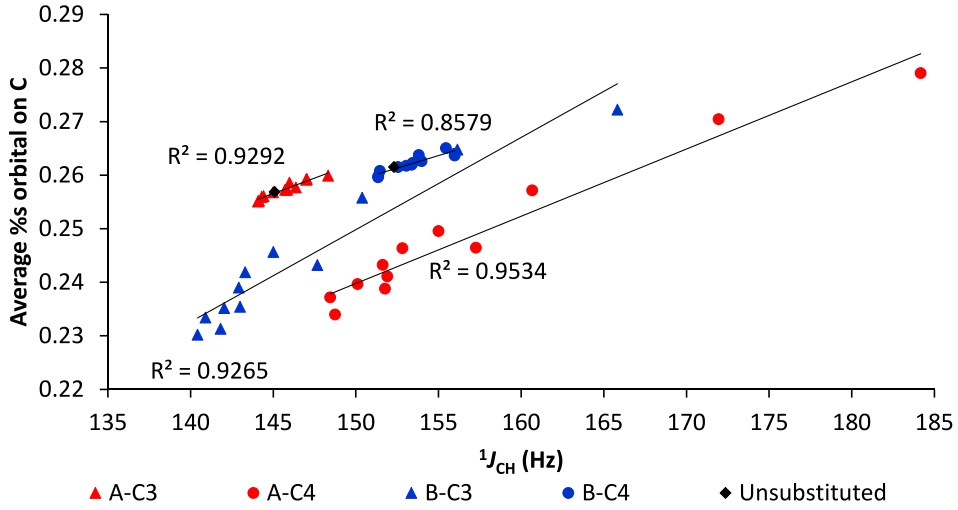

FIGURE 7 $^{1}J_{CH}$ values for the C4 and C3 atoms in each analog compared to the average %s orbital on the carbon.

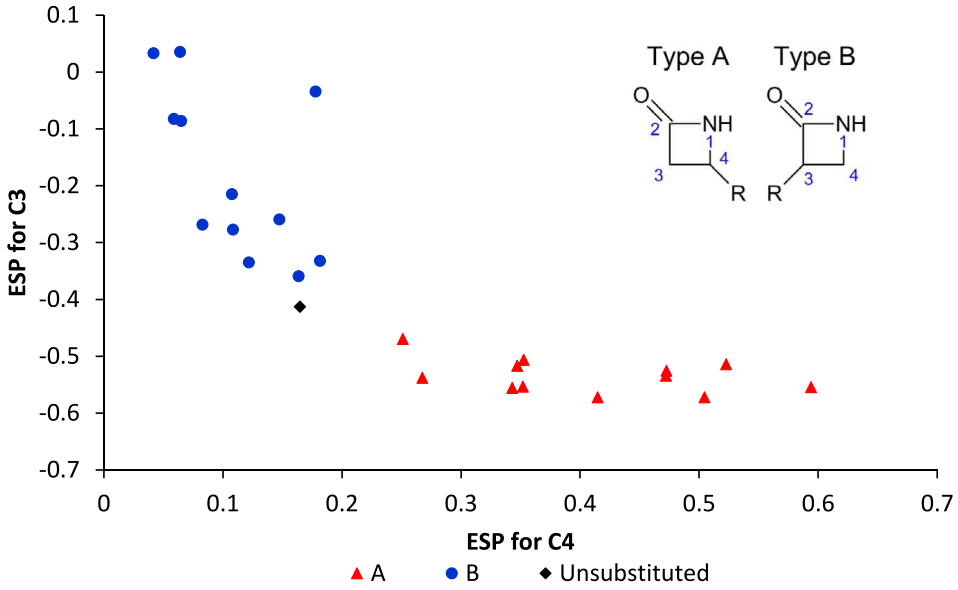

FIGURE 8 ESPs for the C3 and C4 atoms from each of the analogs shown in Figure 1.

7 | DISPARITY IN $^{2}J_{HH}$ BETWEEN TYPE A AND B COMPOUNDS

The most readily apparent trend is the significant difference in the magnitude of geminal proton coupling constants ($^{2}J_{HH}$) on C3 in Type A versus C4 in Type B compounds. The correlation between the ESP and the $^{2}J_{HH}$ is also consistent with our observations regarding the $^{1}J_{CH}$ coupling constants. The $^{2}J_{HH}$ couplings on C3 of Type A compounds are much smaller than the corresponding couplings on C4 of Type B, consistent with more negative ESP on C3 in comparison with the one on C4 (Figure 11). The upfield shift of the methylene protons in A versus B is also consistent with more negative charge on C3 in Type A compounds. It is notable, that the R-group substitution does not have any significant influence on $^{2}J_{HH}$ coupling as opposed to the $^{1}J_{CH}$ couplings. As it has been shown previously,[23,24] the description of $^{2}J_{HH}$ couplings should include the effect of the adjacent electronegative atom, such as nitrogen in this case, on the energy gap between LUMO-HOMO orbitals.

8 | DISPARITY IN $^{2}J_{CH}$ COUPLING CONSTANTS BETWEEN TYPES A AND B COMPOUNDS

The $^{2}J_{CH}$ coupling constants are influenced by a host of factors, including bond angle, and the presence of

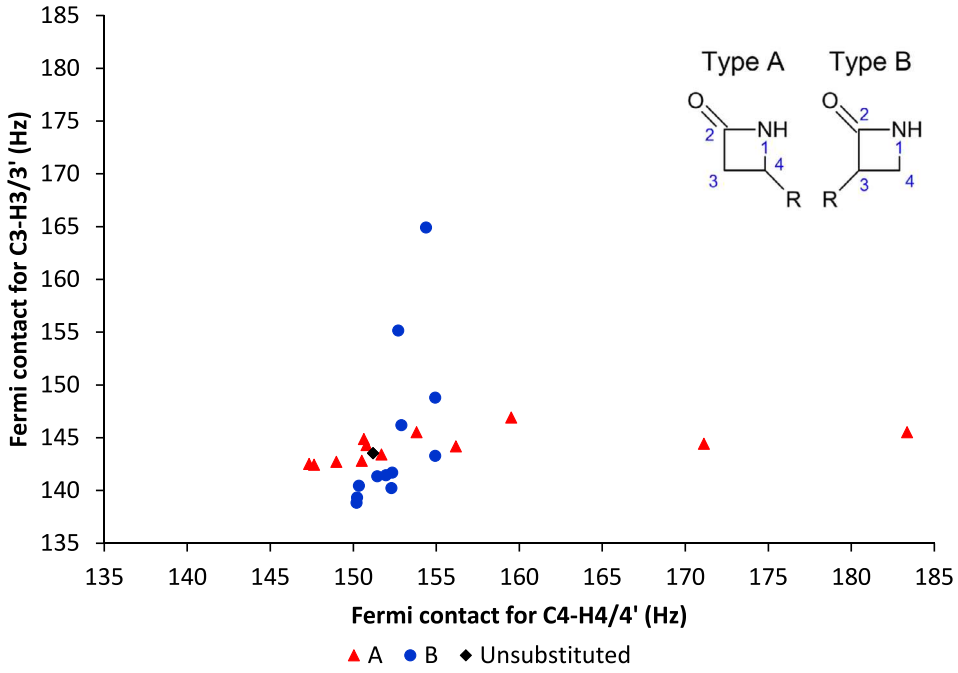

FIGURE 9 The Fermi contacts for the two types of protonated carbons. Note that CH_2 (C3 for Types A and C4 for Type B) values are much more tightly grouped than the CH (C4 for Type A and C3 for Type B). The unsubstituted compound is located at the cross of the two substitution patterns.

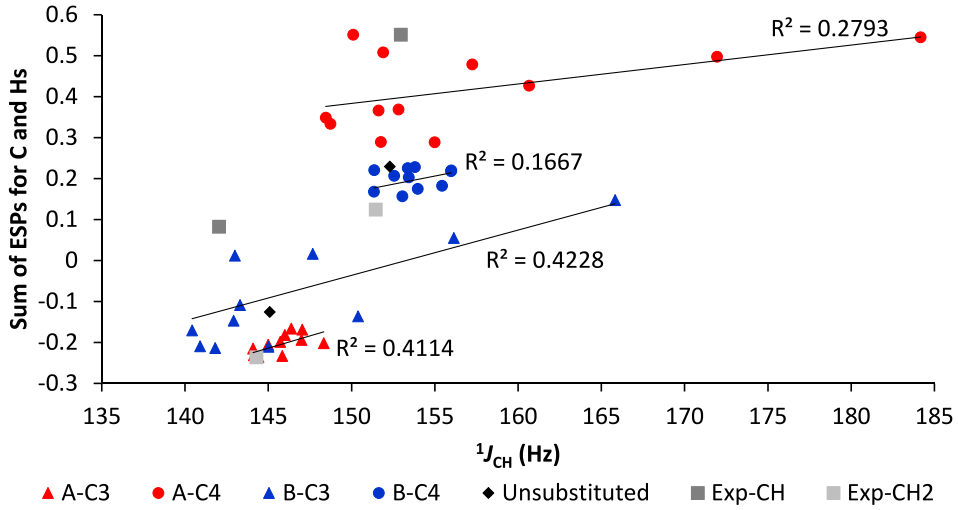

FIGURE 10 The sum of the ESPs at the carbon and its hydrogens versus the DFT-calculated and experimentally measured for R = Me (see Figure 1) $^1J_{CH}$ couplings. Values for methylenes are averaged. The two widely separated points for A-C4 and B-C3 represent cases where an O atom intercedes the R-group and the ring. The R^2 values do not include the experimental data.

electronegative substitution neighboring vicinal carbon atoms.[25–29] This attribute has been broadly used in *J*-based configurational analysis.[25–29] Mainly applied for sp^3-hybridized carbon atoms, a set of Karplus-type equations has been proposed, which also included electronic effects of substituted groups.[30] In case of the β-lactams described in the current study, the $^2J_{CH}$ couplings with the C2 sp^2-hybridized carbon represent a special case that would require a more detailed analysis that will not be addressed in the current study. As far as the $^2J_{CH}$ couplings between H3 and C4 and between H4 and C3, we should report that the observed values in the range −5 to 0 Hz are consistent with Karplus-type curves.[31] The minor dependences of the $^2J_{CH}$ from electronegativities on the adjacent atoms was consistent with earlier observations[29] and the dependences on ESP found in the current study (see the supporting information).

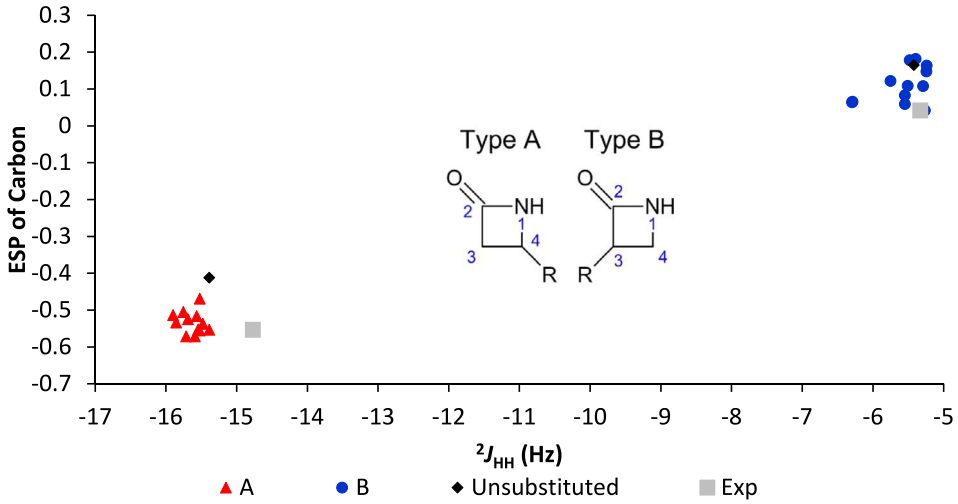

FIGURE 11 The correlation of the ESP of the methylene carbon versus the DFT-calculated and experimentally measured for R = Me (see Figure 1) $^2J_{HH}$ couplings.

9 | CONCLUSIONS

β-lactams remain important pharmaceutical compounds with antibiotic functions, and better understanding of their properties is imperative. The *J* coupling trends can be summarized as follows: the $^1J_{CH}$ coupling for C4 is generally larger than that of C3; the magnitude of the $^2J_{CH}$ coupling between C2 and H3/H3′ is always greater than $^2J_{CH}$ between C4 and H3/H3′; and the geminal coupling of the C3 protons in Type A molecules is always larger than that of C4 in Type B compounds. Analysis of these disparities leads to some overarching conclusions. While all three types of *J* couplings examined in this work correlate very well to the Fermi contact, the Fermi contact itself is determined by multiple factors, including hybridization, electronegativity of substituents, and stereoelectronic effects. The changes in the $^1J_{CH}$ couplings are caused by the differences in the electronic environment, as the trends correlate with the ESP and %s orbital character. Alternatively, the $^2J_{CH}$ couplings do not correlate with the ESP, but they mainly depend on torsion angles and then from the electronegativity of adjacent groups and atoms. Future work will focus on observing whether the trends observed for β-lactams are consistent with other lactam-like groups, such as lactones and thiolactams, and how those trends would be affected by ring size.

ACKNOWLEDGMENTS

The authors would like to thank Drs. Xiao Wang and Ryan Cohen for helpful discussion and Drs. Caroline McGregor, Douglas Richardson, and Edward Sherer from Analytical Research & Development at Merck & Co., Inc., Rahway, NJ, United States, and Drs. Raghavendra Kovvuri and Virendra Tiwari at TCG GreenChem, Inc., for support. National Science Foundation grant numbers CHE0821552 and CHE2116395 for the NMR spectrometers utilized in this work is acknowledged.

ORCID

Emily B. Crull https://orcid.org/0000-0003-3839-7579
Alexei V. Buevich https://orcid.org/0000-0002-5968-9151
Gary E. Martin https://orcid.org/0000-0003-0750-3041
R. Thomas Williamson https://orcid.org/0000-0001-7450-3135

REFERENCES

[1] N. Arya, A. Y. Jagdale, T. A. Patil, S. S. Yeramwar, S. S. Holikatti, J. Dwivedi, C. J. Shishoo, K. S. Jain, *Eur. J. Med. Chem.* **2014**, *74*, 619. https://doi.org/10.1016/j.ejmech.2014.01.002

[2] K. Grabrijan, N. Strašek, S. Gobec, *Expert Opin. Ther. Pat.* **2021**, *31*(3), 247. https://doi.org/10.1080/13543776.2021.1865919

[3] C. J. Murray, K. S. Ikuta, F. Sharara, L. Swetschinski, G. Robles Aguilar, A. Gray, C. Han, C. Bisignano, P. Rao, E. Wool, S. C. Johnson, A. J. Browne, M. G. Chipeta, F. Fell, S. Hackett, G. Haines-Woodhouse, B. H. Kashef Hamadani, E. A. P. Kumaran, B. McManigal, R. Agarwal, S. Akech, S. Albertson, J. Amuasi, J. Andrews, A. Aravkin, E. Ashley, F. Bailey, S. Baker, B. Basnyat, A. Bekker, R. Bender, A. Bethou, J. Bielicki, S. Boonkasidecha, J. Bukosia, C. Carvalheiro, C. Castañeda-Orjuela, V. Chansamouth, S. Chaurasia, S. Chiurchiù, F. Chowdhury, A. J. Cook, B. Cooper, T. R. Cressey, E. Criollo-Mora, M. Cunningham, S. Darboe, N. P. J. Day, M. de Luca, K. Dokova, A. Dramowski, S. J. Dunachie, T. Eckmanns, D. Eibach, A. Emami, N. Feasey, N. Fisher-Pearson, K. Forrest, D. Garrett, P. Gastmeier, A. Z. Giref, R. C. Greer, V. Gupta, S. Haller, A. Haselbeck, S. I. Hay, M. Holm,

S. Hopkins, K. C. Iregbu, J. Jacobs, D. Jarovsky, F. Javanmardi, M. Khorana, N. Kissoon, E. Kobeissi, T. Kostyanev, F. Krapp, R. Krumkamp, A. Kumar, H. H. Kyu, C. Lim, D. Limmathurotsakul, M. J. Loftus, M. Lunn, J. Ma, N. Mturi, T. Munera-Huertas, P. Musicha, M. M. Mussi-Pinhata, T. Nakamura, R. Nanavati, S. Nangia, P. Newton, C. Ngoun, A. Novotney, D. Nwakanma, C. W. Obiero, A. Olivas-Martinez, P. Olliaro, E. Ooko, E. Ortiz-Brizuela, A. Y. Peleg, C. Perrone, N. Plakkal, A. Ponce-de-Leon, M. Raad, T. Ramdin, A. Riddell, T. Roberts, J. V. Robotham, A. Roca, K. E. Rudd, N. Russell, J. Schnall, J. A. G. Scott, M. Shivamallappa, J. Sifuentes-Osornio, N. Steenkeste, A. J. Stewardson, T. Stoeva, N. Tasak, A. Thaiprakong, G. Thwaites, C. Turner, P. Turner, H. R. van Doorn, S. Velaphi, A. Vongpradith, H. Vu, T. Walsh, S. Waner, T. Wangrangsimakul, T. Wozniak, P. Zheng, B. Sartorius, A. D. Lopez, A. Stergachis, C. Moore, C. Dolecek, M. Naghavi, *Lancet* **2022**, *399*(10325), 629. https://doi.org/10.1016/S0140-6736(21)02724-0

[4] J. F. Fisher, S. Mobashery, *Mar. Drugs* **2023**, *21*(2), 86. https://doi.org/10.3390/md21020086

[5] K. D. Barrow, T. M. Spotswood, *Tetrahedron Lett.* **1965**, *6*(37), 3325. https://doi.org/10.1016/S0040-4039(01)89203-0

[6] R. C. Cookson, T. A. Crabb, J. J. Frankel, J. Hudec, *Tetrahedron* **1966**, *22*(SUPPL. 7), 355. https://doi.org/10.1016/S0040-4020(01)99123-9

[7] R. Cahill, R. C. Cookson, T. A. Crabb, *Tetrahedron* **1969**, *25*(19), 4681. https://doi.org/10.1016/S0040-4020(01)83012-X

[8] S. P. Gunasekera, M. Gunasekera, P. McCarthy, *J. Org. Chem.* **1991**, *56*(16), 4830. https://doi.org/10.1021/jo00016a006

[9] M. N. Masuno, I. N. Pessah, M. M. Olmstead, T. F. Molinski, *J. Med. Chem.* **2006**, *49*(15), 4497. https://doi.org/10.1021/jm050708u

[10] D. S. Dalisay, B. I. Morinaka, C. K. Skepper, T. F. Molinski, *J. Am. Chem. Soc.* **2009**, *131*(22), 7552. https://doi.org/10.1021/ja9024929

[11] K. S. Watts, P. Dalal, A. J. Tebben, D. L. Cheney, J. C. Shelley, *J. Chem. Inf. Model.* **2014**, *54*(10), 2680. https://doi.org/10.1021/ci5001696

[12] M. J. Frisch, G. W. Trucks, H. B. Schlegel, G. E. Scuseria, M. A. Robb, J. R. Cheeseman, G. Scalmani, V. Barone, G. A. Petersson, H. Nakatsuji, X. Li, M. Caricato, A. V. Marenich, J. Bloino, B. G. Janesko, R. Gomperts, B. Mennucci, H. P. Hratchian, J. V. Ortiz, A. F. Izmaylov, J. L. Sonnenberg, D. Williams-Young, F. Ding, F. Lipparini, F. Egidi, J. Goings, B. Peng, A. Petrone, T. Henderson, D. Ranasinghe, V. G. Zakrzewski, J. Gao, N. Rega, G. Zheng, W. Liang, M. Hada, M. Ehara, K. Toyota, R. Fukuda, J. Hasegawa, M. Ishida, T. Nakajima, Y. Honda, O. Kitao, H. Nakai, T. Vreven, K. Throssell, J. A. Montgomery, J. E. Peralta, F. Ogliaro, M. J. Bearpark, J. J. Heyd, E. N. Brothers, K. N. Kudin, V. N. Staroverov, T. A. Keith, R. Kobayashi, J. Normand, K. Raghavachari, A. P. Rendell, J. C. Burant, S. S. Iyengar, J. Tomasi, M. Cossi, J. M. Millam, M. Klene, C. Adamo, R. Cammi, J. W. Ochterski, R. L. Martin, K. Morokuma, O. Farkas, J. B. Foresman, D. J. Fox, *Gaussian 16, Revision C.01*, Gaussian, Inc., Wallingford, CT **2019**.

[13] M. W. Lodewyk, M. R. Siebert, D. J. Tantillo, *Chem. Rev.* **2012**, *112*(3), 1839. https://doi.org/10.1021/cr200106v

[14] R. D. Cohen, J. S. Wood, Y.-H. Lam, A. V. Buevich, E. C. Sherer, M. Reibarkh, R. T. Williamson, G. E. Martin, *Molecules* **2023**, *28*(6), 2449. https://doi.org/10.3390/molecules28062449

[15] J. B. Foresman, Æ. Frisch, *Exploring Chemistry with Electronic Structure Methods*, Gaussian, Inc., Wallingford, CT **2015**.

[16] L. Castañar, J. Saurí, R. T. Williamson, A. Virgili, T. Parella, *Angew. Chemie - Int. Ed.* **2014**, *53*(32), 8379. https://doi.org/10.1002/anie.201404136

[17] W. Kutzelnigg, *Theor. Chim. Acta* **1988**, *73*(2–3), 173. https://doi.org/10.1007/BF00528203

[18] J. E. del Bene, J. Elguero, *Chem. Phys. Lett.* **2003**, *382*(1–2), 100. https://doi.org/10.1016/J.CPLETT.2003.10.006

[19] S. A. Perera, R. J. Bartlett, *Mol. Phys.* **2006**, *104*(13–14), 2403. https://doi.org/10.1080/00268970600668587

[20] B. J. Deppmeier, A. J. Driessen, T. Hehre, W. J. Hehre, P. Klunzinger, S. Ohlinger, J. Schnitker, *Spartan'18*, Wavefunction, Inc., Irvine, CA **2019**.

[21] L. B. Krivdin, *Prog. Nucl. Magn. Reson. Spectrosc.* **2018**, *108*, 17. https://doi.org/10.1016/j.pnmrs.2018.10.002

[22] G. E. Maciel, J. W. McIver, N. S. Ostlund, J. A. Pople, *J. Am. Chem. Soc.* **1970**, *92*(15), 4506. https://doi.org/10.1021/ja00718a002

[23] G. A. Aucar, *Concepts Magn. Reson. Part a Bridg Educ. Res.* **2008**, *32*(2), 88. https://doi.org/10.1002/cmr.a.20108

[24] J. A. Pople, A. A. Bothner-By, *J. Chem. Phys.* **1965**, *42*(4), 1339. https://doi.org/10.1063/1.1696119

[25] P. E. Hansen, *Prog. Nucl. Magn. Reson. Spectrosc.* **1981**, *14*(4), 175. https://doi.org/10.1016/0079-6565(81)80001-5

[26] G. Miyazima, Y. Utsumi, K. Takahashi, *J. Phys. Chem.* **1969**, *73*(5), 1370. https://doi.org/10.1021/j100725a033

[27] N. Matsumori, D. Kaneno, M. Murata, H. Nakamura, K. Tachibana, *J. Org. Chem.* **1999**, *64*(3), 866. https://doi.org/10.1021/JO981810K/SUPPL_FILE/JO981810K_S.PDF

[28] R. H. Contreras, J. E. Peralta, *Prog. Nucl. Magn. Reson. Spectrosc.* **2000**, *37*(4), 321. https://doi.org/10.1016/S0079-6565(00)00027-3

[29] G. Bifulco, P. Dambruoso, L. Gomez-Paloma, R. Riccio, *Chem. Rev.* **2007**, *107*(9), 3744. https://doi.org/10.1021/CR030733C/ASSET/IMAGES/LARGE/CR030733CF00027.JPEG

[30] M. Eberstadt, G. Gemmecker, D. F. Mierke, H. Kessler, *Angew. Chemie Int. Ed. English* **1995**, *34*(16), 1671. https://doi.org/10.1002/ANIE.199516711

[31] M. Karplus, *J. Am. Chem. Soc.* **1963**, *85*(18), 2870. https://doi.org/10.1021/ja00901a059

SUPPORTING INFORMATION

Additional supporting information can be found online in the Supporting Information section at the end of this article.

How to cite this article: E. B. Crull, A. V. Buevich, G. E. Martin, R. Mahar, B. Qu, C. H. Senanayake, T. F. Molinski, R. T. Williamson, *Magn Reson Chem* **2024**, *62*(8), 573. https://doi.org/10.1002/mrc.5444